Journal of Ginseng Research 48 (2024) 616–626

Contents lists available at ScienceDirect

Journal of Ginseng Research

journal homepage: www.sciencedirect.com/journal/journal-of-ginseng-research

Research Article

Stem-and-leaf of new hydroponically-cultured ginseng cultivar K-1: A sustainable and innovative resource of ginsenosides for anti-inflammatory agents

Minh Ha Le [a], Ye Hyang Ahn [b], Hyo-Jun Lee [a], Yeon Ju Kim [a,*]

[a] Graduate School of Biotechnology, and College of Life Science, Kyung Hee University, Gyeonggi-do, Republic of Korea
[b] Gyeonggi-do Agricultural research & Extension Services, Gyeonggi-do, Republic of Korea

ARTICLE INFO

Keywords:
Aerial extracts
Anti-Inflammation
Ginsenosides
Hydroponic-cultured ginseng cultivars

ABSTRACT

Background: Korean ginseng (*Panax ginseng* Meyer), a traditional medicine plant cultivated in eastern Asia, has recently captured attention for its potential advancements in hydroponic cultivation, offering a sustainable and innovative resource. Additionally, in the typical processing of ginseng, stem-and-leaf are commonly discarded, leading to resource wastage and overlooking their economically valuable potential as an alternative to the conventionally prioritized roots.

Methods: Initially, we investigated the phenotype of five Korean hydroponically cultivated ginseng cultivars, namely Kumpoong (KP), Chunpoong (CP), Honkaejong (HKJ), Yunpoong (YP), and K-1. Subsequently, we focused on evaluating aerial extracts to identify the most suitable cultivar for reliable resources. This involved phytochemical compositions and anti-inflammatory effects in LPS-stimulated RAW264.7 macrophages and LPS-induced mice, employing quantitative real-time PCR, ELISA, and western blotting.

Results: The K-1 cultivar exhibited superior phenotypic traits and pathogen resistance. HPLC results revealed that aerial extracts contained four times higher ginsenoside content and exhibited a considerable abundance of ginsenoside Rd compared to root extracts. K-1 aerial extract exhibited the highest phytochemical content. The aerial extract of CP and K-1 exhibited greater efficacy in attenuating ROS production, mitigating mitochondrial dysfunction, and reducing pro-inflammatory cytokines (IL-6, TNF-α, iNOS) through the NF-κB and MAPKs signaling pathways, which were corroborated *in vivo* at a 50 mg/kg dose.

Conclusions: Our findings propose the stem-and-leaf of hydroponically cultivated ginseng cultivar K-1 presents an economical alternative to the traditionally valued ginseng root, given its superior stem-and-leaf phenotype and phytochemical content in the aerial extract coupled with promising potential for anti-inflammatory agents in dietary interventions.

1. Introduction

Korean ginseng (*Panax ginseng* Meyer) is a traditional medicinal plant widely cultivated in East Asia, with a history dating back thousands of years [1]. *P. ginseng* is renowned for its potential health benefits to alleviate inflammation-related diseases such as anti-obesity [2], cardiovascular disease [3] and gastrointestinal disorders [4]. Generally, the use of ginseng root in traditional medicine for inflammation treatment has a long-standing history. However, it requires a significant amount of time cultivated in soil before qualifying for commercial use. Additionally, during cultivation, there are multiple obstacles to its maturation, including infectious diseases from soil, accumulation of heavy metals and pesticides, partially loss the yield because of environment impacts, such as heat and salt stress, and global warming [5]. Hydroponic systems have been developed for short-term ginseng cultivation to overcome these disadvantages and have emerged as a promising alternative.

While traditional ginseng roots are renowned for their pharmacological effects, attention has increasingly shifted to the aerial part, including stems and leaves. Notably, these aerial components exhibit a significantly higher total saponin content compared to the roots, despite maintaining a consistent chemical composition [6]. Therefore, ginseng stems and leaves, with their abundant annual output and economic accessibility, are gaining recognition as medicinal vegetables and dietary health supplements [7]. The hydroponic cultivation of ginseng,

* Corresponding author. Graduate School of Biotechnology, and College of Life Science, Kyung Hee University, Yongin-si, 17104, Gyeonggi-do, Republic of Korea.
E-mail addresses: lehaminh2311@khu.ac.kr (M.H. Le), yha062@gg.go.kr (Y.H. Ahn), gy9707@khu.ac.kr (H.-J. Lee), yeonjukim@khu.ac.kr (Y.J. Kim).

https://doi.org/10.1016/j.jgr.2024.07.001
Received 3 January 2024; Received in revised form 9 July 2024; Accepted 9 July 2024
Available online 20 July 2024

with its advantages in productivity [8], offers a sustainable and easily accessible resource to meet the growing demand in global markets. Despite the acknowledged benefits, the specific physiological advantages of hydroponically grown ginseng remain unclear. Additionally, the disparity in ginsenoside and bioactive composition between the stem-and-leaf and root parts of hydroponically grown ginseng is not well-defined. This underscores the necessity for comprehensive studies of these new ginseng resources to fully understand their potential for both phytomedicines and culinary applications.

Inflammation is an important physiological homeostatic response of the innate system to hazardous stimuli and pathogens [9]. Numerous studies highlighted the pivotal role of inflammation in the genesis of chronic pathologies [10]. Recently, heightened attention has been directed towards ginseng dietary interventions, emphasizing their potential anti-inflammatory effects through the reduction of oxidative stress and inflammation biomarkers [11]. Hence, identifying optimal ginseng cultivars for reliable and large-scale production, while considering characteristics, and anti-inflammatory effects, is crucial.

Numerous ginseng cultivars have been developed to exploit its remarkable potential benefits. These cultivars, including Kumpoong (KP), Chunpoong (CP), Honkaejong (HKJ), Yunpoong (YP), and new K-1 cultivar, exemplify the diverse characteristics of *P.ginseng*, such as disease resistance, phenotypic diversity, and high saponin content. In Korea, *P. ginseng* has three primary varieties: Jakyung, Chungkyung, and Hwangsook [12]. CP, the first cultivar officially registered with the Korea Seed and Variety Service, was selected from the Chungkyung variant [13,14]. K-1 and YP originated from Jakyung, while KP was selectively bred from Hwangsook [12,15]. CP is characterized by its light violet stem and orange-yellow berries, exhibiting tolerance to root rust but yielding low productivity [16]. KP, which lacks purple in the stems and has yellow berries, also shows resistance to root rust [17]. K-1 is renowned for its superior root shape and effective disease resistance [18]. YP, bred for high yield and suitable for mass production, is susceptible to rusty root [19]. Despite local landraces and native mixed lines being the most commonly cultivated in Korea, these mentioned cultivars represent only 14.6 % of ginseng fields [20]. HKJ, although not a registered cultivar, is a native mixed line widely cultivated on local farms and commonly sold in Korean markets. Taken together, these five cultivars provide a relevant and practical subset for investigating in this study.

The present study focused on evaluating phytochemical properties including ginsenosides content of aerial and root extracts from five hydroponically grown ginseng cultivars (CP, KP, HKJ, K-1, and YP). Subsequently, we chose two dominant aerial extracts to investigate the underlying anti-inflammatory molecular mechanisms in LPS-stimulated RAW264.7 cells and LPS-induced mouse model.

2. Materials and methods

2.1. Reagents

Dulbecco's modified Eagle's medium (DMEM), penicillin-streptomycin, and fetal bovine serum (FBS) were purchased from GenDEPOT. Lipopolysaccharide (LPS), 2 N Folin & Ciocalteu's phenol reagent, dinitro salicylic acid, 3-(4,5-Dimethylthiazol-2-yl)-2,5-diphenyltetrazolium bromide (MTT), dimethyl sulfoxide (DMSO), and dexamethasone (DEX) were supplied by Sigma-Aldrich. Antibodies of p38, p-p38, ERK, *p*-ERK, JNK, *p*-JNK, NFκB, *p*-NFκB, IκBα, *p*-IκBα were provided by Cell Signaling Technology (Danvers, MA, USA), and β-actin was obtained from Abcam (Cambridge, UK). Secondary antibodies against anti-mouse/rabbit IgG for IP (HRP) were obtained from Thermo Fisher Scientific. Gene primer sequences of iNOS, IL-6 and TNF-α was designed by Macrogen (Seoul, South Korea). All other chemicals were purchased from commercial companies.

2.2. Phenotyping experiment

The phenotyping experiment was conducted at Gyeonggido Agricultural Research and Extension Services, Gyeonggi, Korea (latitude 38°05′00′′N, longitude 127°04′35′′E, altitude 59 m. Voucher specimens (K-1 – 3949, YP – 329, KP – 512, and CP – 318) were deposited in the same department. Five ginseng cultivars were cultivated in a greenhouse using hydroponic method under the controlled environmental conditions. Each cultivar consisted of 30 plants, distributed across three blocks, correspoding as three replicates. Each block was contained 40 L of ginseng hydroponic culture media. The greenhouse maintained an average temperature of 27.4 °C, humidity at 45 %, and provided lighting for 16 h, with a specific LED light ratio of 2 blue parts (450 nm): 1 green part (520 nm): 4 part red (660 nm), delevering a light intensity of 60–100 μmol m^{-2} s^{-1}. The sample size remained consistent, as one-year-old ginseng seedlings were used in this study. Morphological traits, such as aerial length, leaf length, stem length, stem width, leaf width, root length, root width, fresh weight of aerial and root part, were determined after 40 days of cultivation. The measurement of those traits was described in Fig. S1. Pathogenic infections in plant root systems have been documented. The symptoms initially appeared as brown lesions, which subsequently increased in size and changed to black color. **2.3. Plant material and preparation**.

The five cultivars were separated into aerial and root parts, lyophilized, and ground into powder after washing. Each lyophilized powder (1 g) was extracted twice with 20 mL of 80 % methanol for 1 h at 80 °C in a reflux system. The extract was filtered and concentrated using a rotary evaporator at 50 °C. 20 mL of distilled water was used to dissolve the residue, which subsequently was freeze-dried and stored at – 50 °C for further experiments.

2.3. HPLC analysis

2.3.1. Sample preparation

After collecting the residue of each sample from refluxing two times with 80 % methanol, as described above, the residue was dissolved in 20 mL of distilled water, 20 mL of water-saturated *n*-butanol was added, and the mixture was shaken vigorously. The sample was centrifuged at 5000×*g* for 15 min, and the butanol fraction was evaporated at 50 °C on the same rotary evaporator. The residue was dissolved in 80 % methanol and filtered through a 0.45 μm filter before HPLC analysis.

2.3.2. HPLC analysis

The ginsenosides content was determined using an Agilent 1260 series HPLC system (Palo Alto, CA, USA). This experiment employed a C18 column (250 mm × 4.6 mm, 5 μm) using distilled water (solvent A) and acetonitrile (solvent B) in mobile phages with a flow rate of 1.6 mL/min. The following gradient was followed: 19.5 % B (0–29 min), 30 % B (29–36 min), 32 % B (36–45 min), 34 % B (45–47 min), 35.5 % B (47–49 min), 100 % B (49–61 min), 19.5 % B (61–66 min). Ginsenoside composition was detected at a wavelength of 203 nm.

2.4. Chemical component analysis

2.4.1. Determination of total flavonoid content measurement

The aluminum chloride method determined total flavonoid content. Briefly, 100 μL of ginseng aerial and root extracts (1 mg/mL) was added to 10 μL of 80 % ethanol. Then, 20 μL of 10 % aluminum nitrate and 1 M potassium acetate were added to the mixture, diluting by 150 μL 80 % ethanol immediately. Quercetin was used as a standard for the calibration curve. TFC of samples was calculated as milligrams of quercetin per gram of sample (mg QE/g). Absorbance was measured at 415 nm.

2.4.2. Determination of total polyphenol contents

Total polyphenol content was assessed using the Folin-Ciocalteu method. 10 μL of aerial and root extracts (1 mg/mL) was mixed with

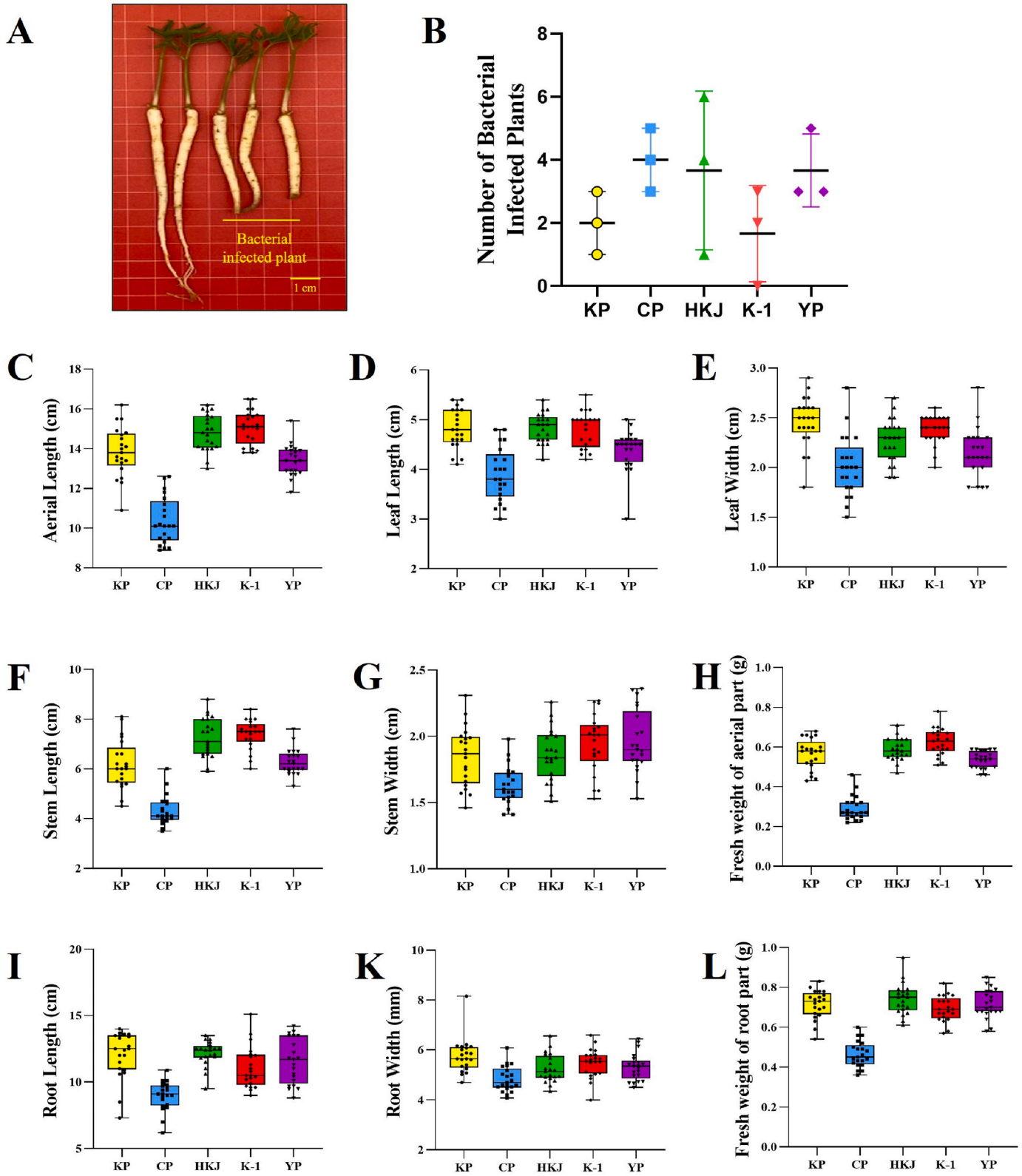

Fig. 1. Phenotype analysis of five hydroponic-cultured ginseng cultivars. The representative pathogen-infected plants compared to healthy plants (A); Pie chart showing the percentage of pathogen infected cultivars (B). Box plots exhibiting phenotypic distribution of aerial length (C), leaf length (D), stem length (E), stem width (F), leaf width (G), fresh weight of aerial part (H), fresh weight of root part (I), root length (K), root width (L).

10 μL of 2 % sodium carbonate. Then, 200 μL of 50 % Folin-Ciocalteu reagent was added and incubated for 1 h. Absorbance was measured at 750 nm. Gallic acid was used as a standard for the calibration curve. Total phenolic content was calculated as milligrams of gallic acid per gram of sample (mg GA/g).

2.4.3. Determination of total protein contents

The Bradford assay was used for the determination of total protein. Briefly, the mixture contained 200 μL of aerial and root extracts (1 mg/mL) and 50 μL of Bio-rad reagent and was then incubated at room temperature (25 ± 2 °C) for 5 min. Absorbance was measured at 600 nm. Bovine serum albumin was used as a standard for the calibration curve. Total protein content was analyzed as milligrams of bovine serum albumin per gram of sample (mg BSA/g).

2.4.4. Determination of reducing sugar

Reducing sugar content was analyzed through the dinitrosalicylic acid (DNS) reagent method. 0.5 mL of aerial and root extracts (1 mg/mL) and 1.5 mL of DNS reagent were mixed and boiled at 100 °C for 15 min. Absorbance was measured at 540 nm after cooling the mixture. Reducing sugar content was analyzed based on calibration curves using glucose as a reference.

2.5. Cell culture

RAW264.7 cell lines were purchased from Korean Cell Line Bank (Seoul National University, Seoul, Korea) and cultured in DMEM with 10 % FBS and 1 % penicillin-streptomycin in an incubator at 37 °C with 5 % CO_2.

2.6. Cell viability assay and nitric oxide determination

The MTT assay was performed to determine the cytotoxicity of the aerial extracts on RAW264.7, which were seeded into 96-well plates at a density of 1.5×10^5 cells/well and incubated for 24 h. After RAW264.7 cells were treated with the aerial extracts at different concentrations (50 and 100 μg/mL), and LPS (1 μg/mL) for 24 h, 100 μL MTT (0.5 mg/mL) reagent was added and incubated for 2 h. Next, 100 μL of DMSO was dissolved, and absorbance was measured at 570 nm using a microplate reader (Molecular Devices Filter Max F5).

Griess reagent was used to measure nitrite levels to analyze NO production. Culture medium (100 μL) was mixed with 100 μL of Griess reagent in a new 96-well plate and incubate for 10 min. The absorbance was measured at 570 nm, and sodium nitrite was used as a standard curve.

2.7. Enzyme-linked Immunoassay (ELISA)

After samples treatment with LPS in RAW264.7 cells as described in section 2.7, 100 μL of cell supernatant was collected to estimate the level of IL-6, IL-1β, and TNF-α using ELISA kit (R&D Systems, Minneapolis, MN, USA) according to manufacturer's instruction.

2.8. Quantification of reactive oxygen species (ROS) and mitochondrial Superoxide (Mito-SOX)

Cells were cultured in 6-well plates (2×10^5 cells/well) and treated with samples and LPS (1 μg/mL) for 24 h, incubated, and measured using the cellular ROS/(Mito-SOX) Detection Assay Kit (Abcam, Cambridge, UK) following manufacturer's protocol to detect the release of ROS and Mito-SOX. Fluorescence was visualized using an LSM 510 and 510 META laser scanning microscopes (Leica).

2.9. Quantitative real-time PCR (qRT-PCR)

Total RNA was extracted using a TRIzol reagent kit (Invitrogen, Carlsbad, CA, USA) and reverse-transcribed into cDNA using an amfiRivert cDNA Synthesis Platinum Enzyme Mix (GenDEPOT). qRT-PCR was conducted according to the manufacturer's instructions using an amfiSure qGreen Q-PCR Master Mix (2 ×) Kit (GenDEOT) on a Rotor-Gene qRT-PCR (QIAGEN, Seoul, Korea). 500 ng cDNA was mixed with 10 μL amfiSure qGreen Q-PCR Master Mix (GenDEPOT) in a final volume of 20 μL. The primer sequences were listed in Table S1.

2.10. Western blotting

RAW264.7 cells, after being treated with appropriate amounts of samples, were collected, and lysed using the RIPA buffer reagent (Thermo Fisher Scientific) containing protease inhibitors (GenDEPOT) for 1 h and then centrifuged at 13,000 rpm for 20 min. After quantifying the protein concentration using Bradford reagent (Sigma-Aldrich), equal amounts (50 μg), were added to 10 % SDS-PAGE using an Invitrogen 2 mini electrophoresis tank system and then transferred to PVDF membranes (Thermo Fisher Scientific). The membranes were blocked with 5 % skim milk at room temperature for 1 h. After washing with PBST 3 times, the membranes were incubated overnight at 4 °C with the primary antibodies (1:1000 dilution) followed by incubation with the diluted secondary antibody (1:1000) at room temperature (25 ± 2 °C) for 2 h. West-Q Pico ECL Solution (GenDEPOT) was used to visualize protein bands detected using the Alliance MINI HD9 AUTO Immunoblot Imaging System (UVItec Limited, Cambridge, UK). Protein expression levels were quantified using the ImageJ software.

2.11. Animals and in vivo experimental design

Male C57BL/6 (6 weeks old, 19–21 g) were purchased from Orient Bio (Seongnam, South Korea) and group-housed (6 animals per cage) under stable condition (temperature: 23 ± 2 °C, humidity: 50 % ± 10 %, light/dark cycle: 12 h). This study was approved by the Animal Care and Use Guidelines of Kyung Hee University (KHGASP-23-046).

After adaptation one week, mice were divided into five groups: control (CON), model (LPS), positive control (DEX), CP and K-1. The CON and LPS groups received excipients (distilled water), DEX (1 mM), CP and K-1 (50 mg/kg) by gavage once daily for 7 days. On the seventh day, all groups except the CON group were intraperitoneal injected with LPS (2 mg/kg). Body weight was measured daily. At the end of this experiment (8th day), all the mice were anaesthetized, euthanized for organ collection, and weight. A portion of the spleen was fixed with 10 % formalin buffer and embedded in paraffin for hematoxylin and eosin (H&E) staining (Abcam). The remaining splenic tissue were subjected to ELISA and immunoblotting.

2.12. Statistical analysis

All data were expressed as the mean ± standard deviation (SD) of three experimental repeats. GraphPad Prism version 8 (GraphPad Software, Inc.) was used for statistical analysis. Statistical differences between mean values were determined using Student's *t*-test, and $p < 0.05$, $p < 0.01$, and $p < 0.001$ value were considered significant.

3. Results and discussion

3.1. Phenotyping

The high nutrient concentrations in hydroponic cultivation can facilitate the growth of pathogens, such as bacterial soft rot, which commonly affects plant storage organs like tubers or rhizomes, leading to tissue necrosis [21,22]. This pathogenic symptom was recorded in our hydroponic cultured ginseng cultivar, as shown in Fig. 1A. Among the five cultivars, K-1 showed the lowest number of bacterial infected plants, with a mean of 1.7 ± 1.5, while CP exhibited the highest number, averaging 4.0 ± 1.0 infected plants (Fig. 1B). This could be explained by

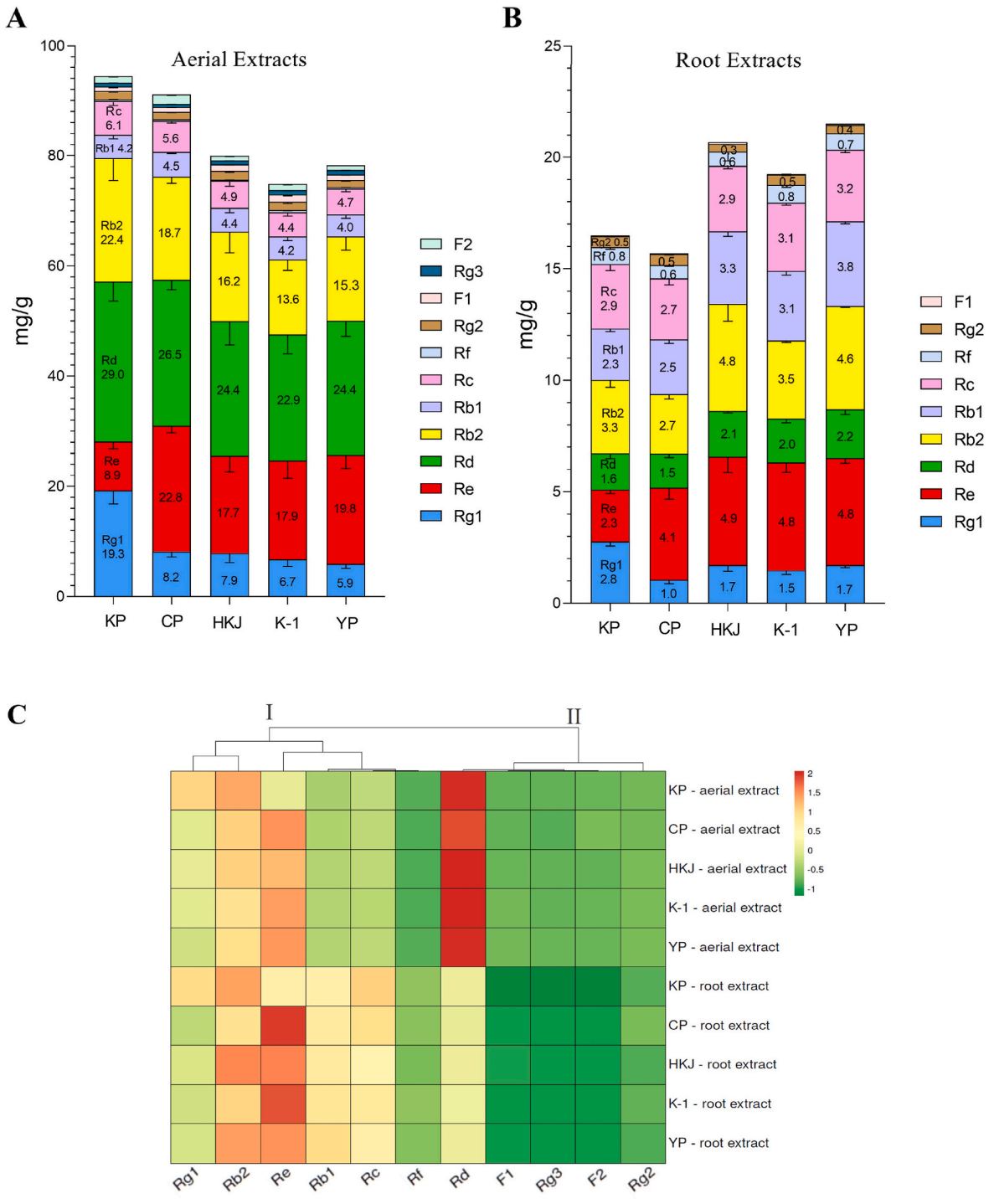

Fig. 2. Ginsenoside properties of aerial and root extracts. Content of ginsenosides identified from aerial extracts (A) and root extracts (B); Heatmap analysis of ginsenoside content (C).

a previous study reported that K-1 had stronger disease resistance owing to its root structure [23].

As the demand for ginseng products increases, phenotypic traits play a significant role in determining productivity. In the present study, the five cultivars exhibited different distributions at nine traits (Fig. 1C–L). The new K-1 cultivar possessed the highest median value of aerial traits including aerial length, leaf length, stem length, stem width, and fresh weight of aerial part. CP, a traditional cultivar, show a high quality over other varieties and gives a high yield and high resistance to ginseng rusty root rot disease in soil cultivation [24]. However, in hydroponic system, CP had the lowest medians of all phenotype characteristics. These results suggested that K-1 cultivar emerged as a highly productive and adaptation cultivar, exhibiting significant value in aerial phenotyping data and pathogen resistance compared to the other cultivars.

3.2. *Ginsenosides composition*

The ginsenoside composition of the aerial and root extracts of the five different cultivars was identified using HPLC analysis. Significant variations were observed in the distribution of ginsenosides between the

Table 1
Total flavonoid, polyphenol, protein, and sugar contents of aerial and root extracts from five ginseng cultivars.

Samples		Flavonoid	Polyphenol	Protein	Sugar	Total
		mg QE/g	mg GA/g	mg BSA/g	mg GE/g	
Arial part	KP	4.1 ± 0.3	35.7 ± 1.4	55.4 ± 0.5	249.5 ± 4.6	344.7
	CP	4.6 ± 0.5	25.5 ± 2.7	57.2 ± 0.8	343.8 ± 9.4	430.8
	HKJ	3.9 ± 0.1	27.9 ± 2.3	45.6 ± 1.0	334.3 ± 6.8	418.2
	K-1	3.7 ± 0.4	44.8 ± 0.2	61.1 ± 0.5	339.4 ± 8.1	449
	YP	3.3 ± 0.2	41.3 ± 4.5	48.3 ± 1.4	287.2 ± 5.0	380.1
Root Part	KP	4.7 ± 0.4	24.4 ± 1.1	51.2 ± 2.6	136.4 ± 8.6	216.6
	CP	4.7 ± 0.3	25.2 ± 5.8	49.2 ± 1.2	161.5 ± 10.0	240.6
	HKJ	5.2 ± 0.3	21.2 ± 2.3	46.1 ± 1.0	167.0 ± 3.0	239.5
	K-1	4.8 ± 0.5	28.5 ± 1.0	49.2 ± 0.7	193.9 ± 8.9	276.4
	YP	4.7 ± 0.5	18.2 ± 1.1	54.3 ± 1.9	144.0 ± 4.4	221.3

root and aerial extracts. Overall, the total ginsenoside content of the aerial extracts was approximately 4-fold higher than that of root extracts (Fig. 2A–B), aligning with consistent trends observed in previous studies [25,26]. Notably, both aerial and root extracts exhibited a spectrum of ginsenosides, including prominent components such as Rg1, Re, Rd, Rb2, Rb1, Rc, as well as minor components like Rf, Rg2, and F1. Interestingly, ginsenoside Rg3 and F2 were exclusively found in the aerial extracts. Among the five aerial extracts, KP demonstrated the highest levels of saponins, specifically for ginsenosides Rg1, Rd, Rb2, and Rc (19.3 ± 2.4, 29.0 ± 3.5, 22.4 ± 4.1, 6.1 ± 0.8 mg/g, respectively). Conversely, in root extracts, YP showed the highest level, with the highest ginsenosides Rd, Rb1, and Rc (2.2 ± 0.2, 3.8 ± 0.1, 3.2 ± 0.1 mg/g, respectively). Additionally, KP aerial and root extracts contained the highest Rg1 content but the lowest Re among cultivars, consistent with previous finding in ginseng berries [27]. A previous study demonstrated that there were variations in ginsenoside content among cultivars due to differences in the characteristics of plants and primary metabolites. These differences leaded to variations in pathways and responses to the external environment factors [28].

The heatmap analysis was conducted to elucidate the relatively clustering of saponins and visualize of the ginsenoside contents across various part extractions of different cultivars. The ginsenoside content of each extract was revealed through color shading, with red indicating high content, green indicating low content. As shown in Figs. 2C and 11 ginsenosides were divided into two major clusters. Cluster I predominantly encompassed abundant ginsenosides such as Rg1, Rb2, Re, Rb1, Rc, and Rf, while cluster II comprised Rd, F1, Rg3, F2, and Rg2. The trend of ginsenoside content variation between aerial and root extracts indicated higher ginsenoside content in cluster I than that in cluster II. Significantly, ginsenoside Rd was the most abundant in aerial extracts. Extensive research has highlighted the pharmacological activities of ginsenoside Rd, including its anti-inflammatory effects by reducing pro-inflammatory cytokines production and ameliorating colitis in mice [29]. Moreover, Rd has been reported to mitigate oxidative stress-induced cell damage by elevating glutathione levels in H4IIE cells via NF-κB-dependent γ-glutamylcysteine ligase induction [30]. Collectively, these findings underscored that the aerial extracts not only contained higher overall ginsenoside content but also exhibited a pronounced abundance of ginsenoside Rd compared to root extracts. This suggests that aerial extracts might serve as a more reliable source for ginsenosides, offering potential benefits for applications in anti-inflammation.

3.3. Phytochemical analysis

Bioactive characterization plays a vital role in the identification and quantification of bioactive compounds in plant-based materials, elucidating their potential health-promoting properties [31]. Particularly, phytochemical analyses uncover the existence of specific phytoconstituents such as polyphenols, flavonoids, alkaloids, and terpenes, which are known to possess various pharmacological, antioxidant, and anti-inflammatory activities [32]. Besides, proteins and carbohydrates, fundamental components of the human diet and primary sources of sustenance for all living organisms [33,34]. Hence, phytochemical screening of aerial and root extracts was performed in this study. Table 1 showed that the aerial extracts exhibited higher bioactive components than root extracts. The aerial extracts of K-1 cultivar had the highest total phytochemical content, followed by CP and HKJ aerial extract. Particularly, K-1 aerial extract possessed the highest level of total polyphenol and protein accounting for 44.8 ± 0.2 mg GA/g, 61.1 ± 0.5 mg BSA/g, respectively. Besides, the root extract of HKJ had the highest content of flavonoids, accounting for 5.2 ± 0.3 mg QE/g. The highest reducing sugar level was exhibited in CP aerial extract (343.8 ± 9.4 mg GE/g). Based on these results, K-1 was the prominent cultivar with the dominant phytochemical content in aerial extracts.

3.4. Cell viability and inhibitory effect on NO production

As the frontline defenders against invading pathogens, macrophages eliminate pathogens by releasing various cytokines and mediators including nitric oxide (NO), a crucial signaling molecule in the early phases of immune response [35,36]. This study initially focused on investigating the cytotoxicity and inhibitory NO production of five aerial extracts in RAW264.7 cells because of their prominent ginsenoside and phytochemical content. In the presence of lipopolysaccharide (LPS) stimulation (1 μg/mL), all samples demonstrated negligible cytotoxicity, maintaining cell viability above 89 % at concentrations of 100 μg/mL, and 1 μM for positive control - dexamethasone (DEX) as depicted in Fig. 3A. Next, the results revealed a significant increase in NO secretion in LPS-treated group compared to control (15.0 ± 0.4 μM). Moreover, the aerial extracts of HKJ, CP, and K-1 considerably decreased NO production compared to KP and YP at a concentration of 100 μg/mL. Particularly, the aerial extract of K-1 proved to be the most potent in reducing the LPS-induced NO release to 4.2 ± 0.5 μM, followed by CP and HKJ with levels of 5.0 ± 0.7 μM, 5.9 ± 0.1 μM, respectively (Fig. 3B). This could be explained based on the phytochemical results of aerial extracts as described in the aforementioned section. Despite the K-1 aerial extract having the lowest total ginsenoside content among the studied ginseng cultivars, it exhibited the highest level of phytochemical components, particularly total polyphenols. Polyphenols exert potent anti-inflammatory effects by inhibiting key inflammatory mediators, particularly in reducing NO release [37]. Consistent with previous report, the fermented and aged mountain-cultivated ginseng sprouts with the highest total phenolic content exhibited stronger anti-inflammatory properties, while their ginsenoside level was the lowest [38]. Furthermore, the ranking of the three aerial extracts (K-1, CP, and HKJ) in terms of their ability to significantly decrease NO production corresponded with their ranking in phytochemical content. This suggested a strong correlation between high phytochemical levels and effective NO reduction. Consequently, based on these findings, CP, HKJ, and K-1 aerial extracts were selected for subsequent experiments.

3.5. Inhibitory effect on LPS-induced pro-inflammatory cytokines

Following LPS stimulation, intracellular signaling pathways were activated and induced pro-inflammatory cytokines such as IL-6 and TNF-α. To evaluate the effect of CP, HKJ, and K-1 aerial extracts on

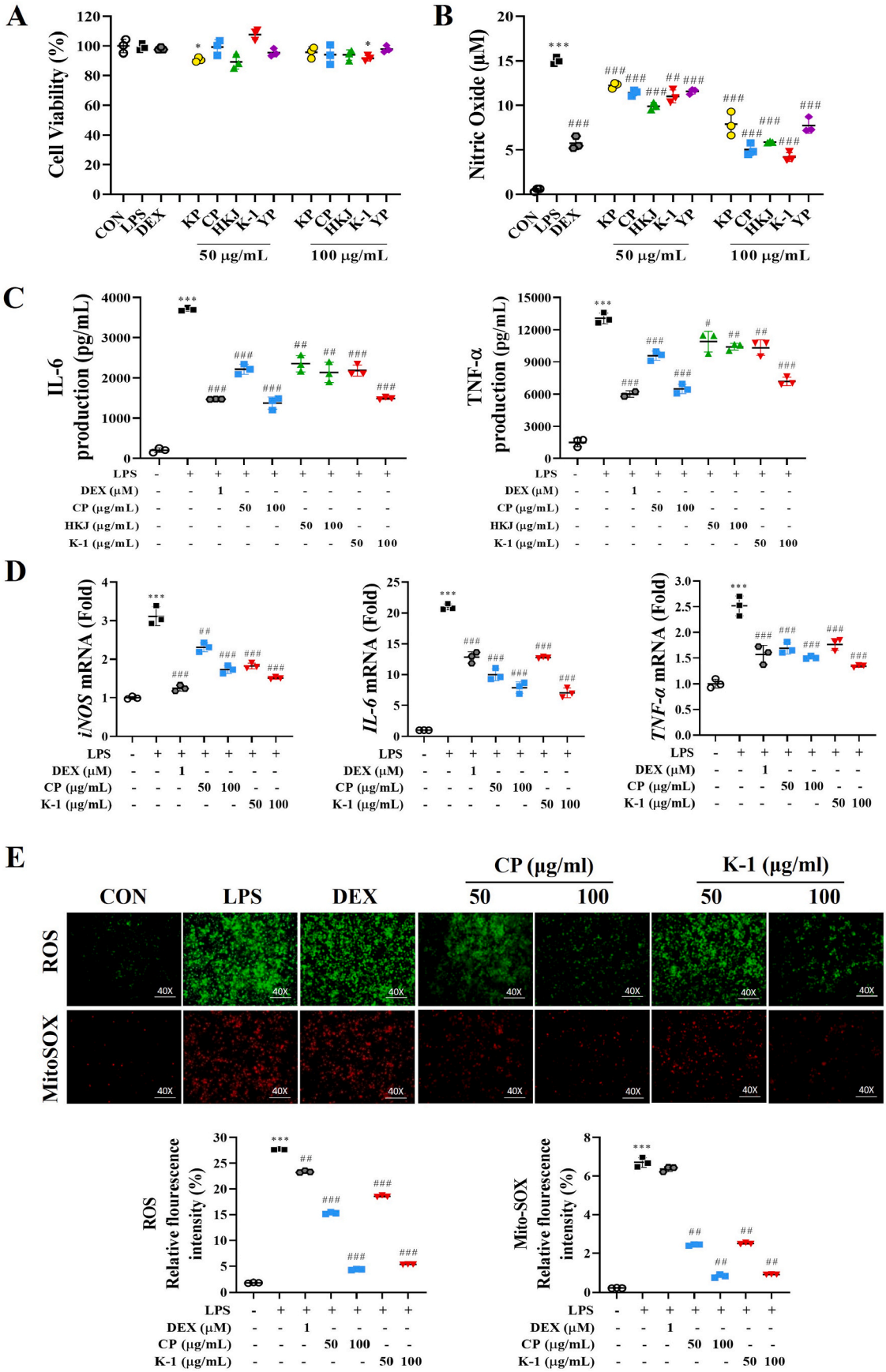

Fig. 3. The effects of aerial extracts treated in LPS-stimulated RAW264.7 cells. Cell viability (A); NO production (B); cytokine secretion (C); cytokine expression (D); ROS production and MitoSOX (E). All values are expressed as mean ± S.D. $^{*}p < 0.05$, $^{**}p < 0.01$, $^{***}p < 0.001$ vs. control group; $^{\#}p < 0.05$, $^{\#\#}p < 0.01$, $^{\#\#\#}p < 0.001$ vs. LPS group.

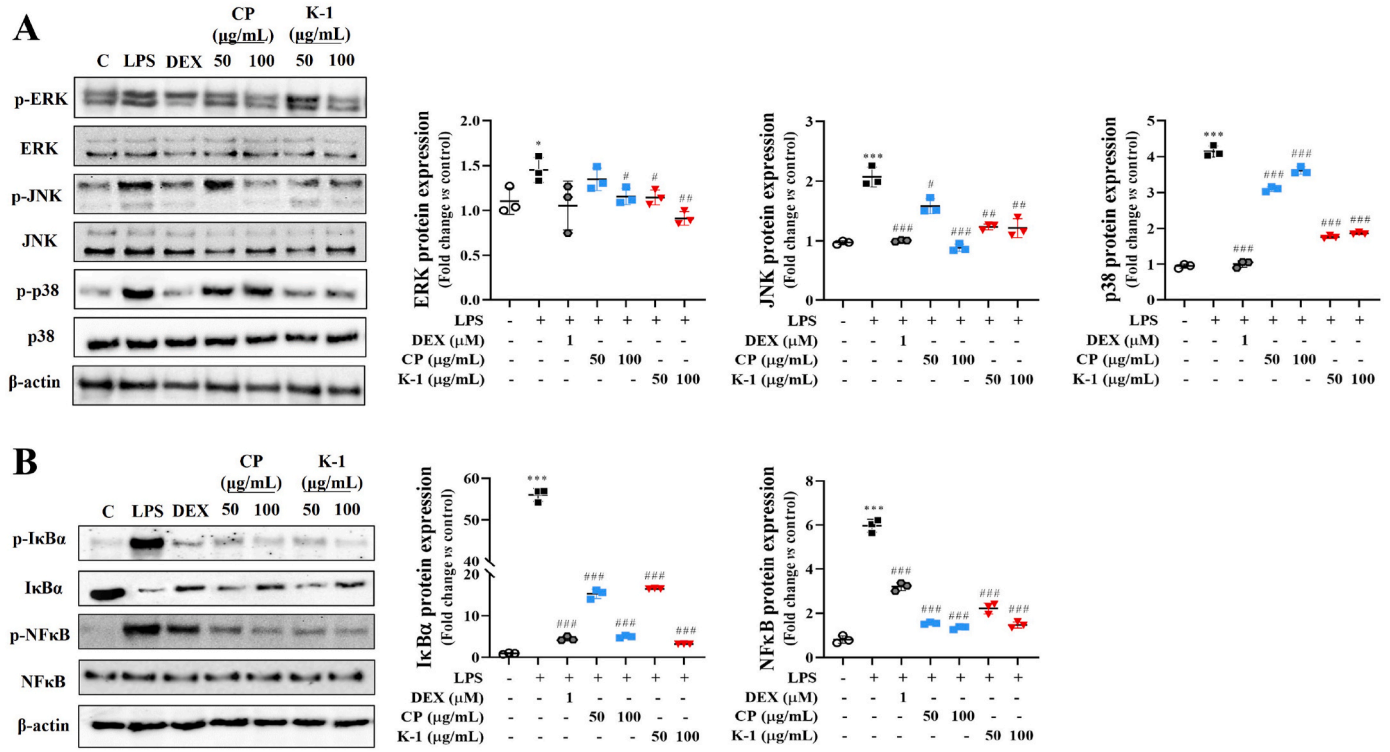

Fig. 4. Western blot analysis of NF-κB and MAPK pathway of CP and K-1 aerial extracts in LPS-stimulated RAW264.7 cells. Western blot analysis of MAPK pathway (A); Western blot analysis of NF-κB signaling pathway (B). All values are expressed as mean ± S.D. $^{*}p < 0.05$, $^{***}p < 0.001$ vs. control group; $^{\#}p < 0.05$, $^{\#\#}p < 0.01$, $^{\#\#\#}p < 0.001$ vs. LPS group.

inflammation, the production of these cytokines was assessed using ELISA. In Fig. 3C, LPS-stimulated RAW264.7 cells showed significantly increased IL-6 and TNF-α levels. However, these productions significantly reduced by CP and K-1 aerial extracts at the concentration of 100 μg/mL ($p < 0.001$), comparable to DEX ($p < 0.001$). Additionally, HKJ aerial extract exhibited a slight reduction compared to the LPS-treated group ($p < 0.01$). Hence, CP and K-1 aerial extracts were chosen for gene expression investigation using qRT-PCR analysis.

The inducible nitric oxide synthase (iNOS) acts as a mediator, upregulating the inflammatory response by catalyzing high levels of NO production [39,40]. To determine the mechanism underlying the suppressive NO production effect of aerial extracts, we assessed the transcriptional levels of *iNOS*, coupled with pro-inflammatory cytokines. Our results revealed that LPS stimulation considerably increased mRNA levels of *iNOS, IL-6*, and *TNF-α*, which were remarkably reduced by CP and K-1 aerial extracts treatment (50–100 μg/mL) in RAW264.7 macrophages (Fig. 3D). These findings suggested that the aerial extracts of CP and K-1 hold promise for their potential mechanisms in down-regulating cytokine release.

3.6. Inhibitory effect on LPS-induced ROS production and mitochondrial Superoxide

ROS, crucial regulators of intracellular signaling and homeostasis, play a significant role in LPS-induced inflammation in macrophages by serving as signaling molecules that activate transcription factors, and leading to the expression of pro-inflammatory mediators and cytokines [41,42]. In this context, we evaluated the impact of CP and K-1 aerial extracts on ROS production and MitoSOX in LPS-stimulated macrophages. As shown in Fig. 3E, the LPS group exhibited a remarkable increase in fluorescence intensity for both ROS (green) and MitoSOX (red) compared to the control group. Notably, treatment with DEX did not inhibit ROS production and MitoSOX expression in RAW264.7 cells induced by LPS, which is consistent with previous studies [43]. However, CP and K-1 aerial extracts significantly decreased the fluorescence intensity of ROS and MitoSOX by over 80 % at the concentration of 100 μg/mL. Moreover, there was no significant difference between CP and K-1 aerial extracts. These results collectively suggested that CP and K-1 aerial extracts possessed the similar capability to suppress the accumulation of LPS-induced ROS in macrophages.

3.7. Inhibitory effect on NFκB and MAPK signaling pathways

The potent pro-inflammatory effects of TNF-α and IL-6 cytokines are primarily mediated through the activation of NFκB and MAPKs signaling pathways [44]. Hence, to further investigate the molecular mechanisms by which CP and K-1 aerial extracts modulate these cytokines, we assessed the protein levels of MAPKs and NFκB signaling pathway components. As demonstrated in Fig. 4A, LPS stimulation significantly increased phosphorylation of the three MAPKs (ERK, JNK, p38 kinase). However, CP and K-1 aerial extracts effectively reduced their phosphorylation without altering overall expression. The NFκB signaling pathway, another crucial pathway involved in the inflammatory response, is activated following MAPKs pathway activation [45]. Upon LPS stimulation, the phosphorylated form of IκBα undergoes ubiquitination and degradation, leading to the nuclear translocation of NFκB and subsequent transcription of inflammatory genes [46]. In this study, phosphorylated of IκBα was significantly increased in LPS-stimulated cells, indicative of IκBα degradation and NFκB complex activation. However, treatment with CP and K-1 aerial extracts down-regulated the phosphorylation of IκBα and NFκB, resulting in their suppression (Fig. 4B). No statistical differences were observed between CP and K-1 aerial extract groups. Our results indicate that the anti-inflammatory effect of CP and K-1 aerial extracts was regulated via the NFκB and MAPKs pathway in LPS-stimulated RAW264.7 macrophages.

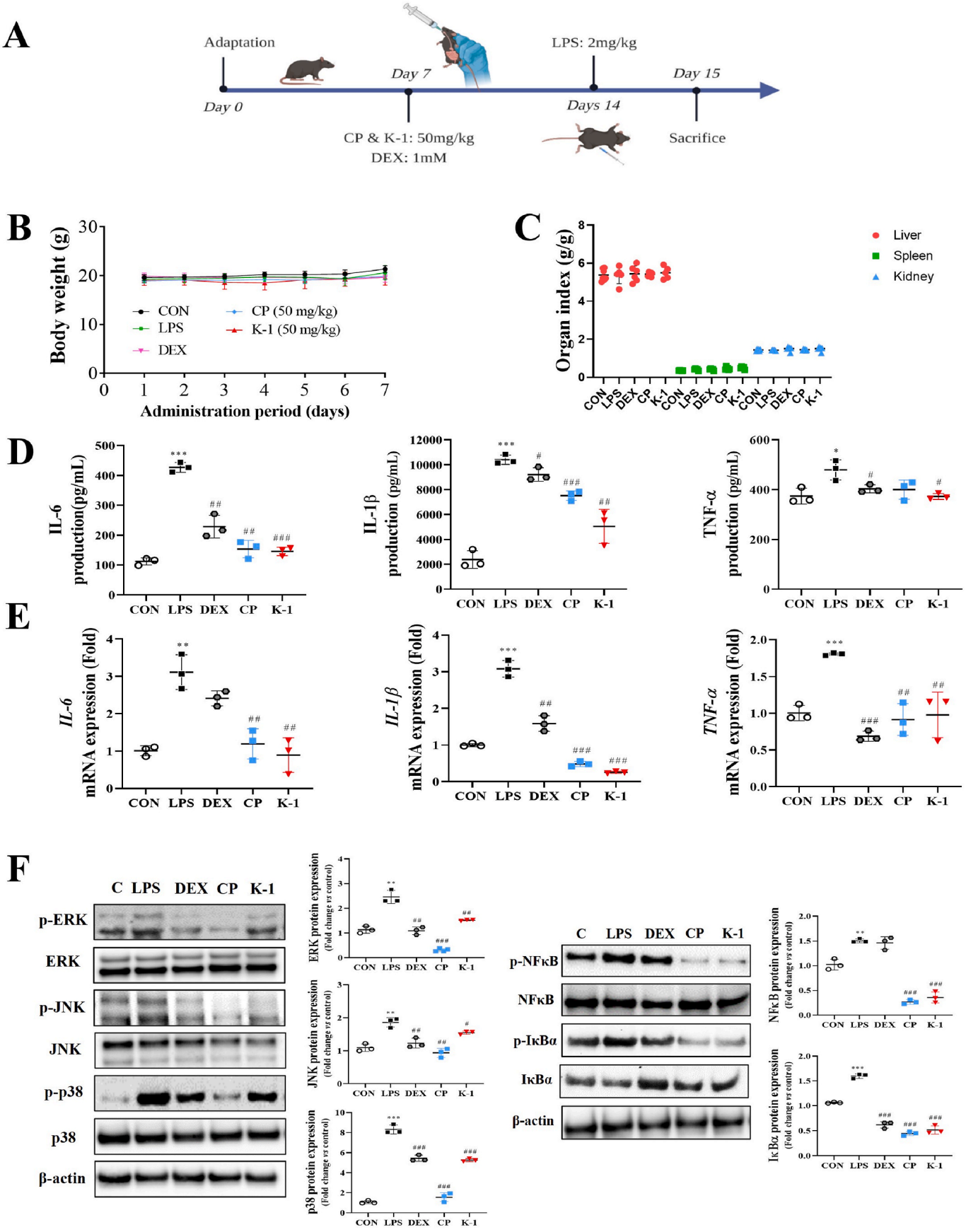

Fig. 5. Effects of CP and K-1 aerial extracts on LPS-induced mice's spleen. Animal experimental design (A); Body weight (B); Organ index (C); Cytokine production of IL-6, IL-1β, and TNF-α (D); Cytokine expression (E) Western blot analysis of NF-κB and MAPKs pathway (F). All values are expressed as mean ± S.D. $^{**}p < 0.01$, $^{***}p < 0.001$ vs. control group; $^{\#}p < 0.05$, $^{\#\#}p < 0.01$, $^{\#\#\#}p < 0.001$ vs. LPS group.

3.8. Anti-inflammatory effect on the LPS-injected mice

Based on *in vitro* results, it was hypothesized that CP and K-1 aerial extracts would exhibit subtantial anti-inflammatory effects in mice subjected to LPS injection. As a positive control, DEX was administered to mice, while the other groups received the respective medications, as illustrated in Fig. 5A. Body weight and organ indices are fundamental indicators of the overall health of mice. During the administration period, no statistically significant differences were observed among the groups in body weight and major organs indices, including the liver, spleen, and kidney (Fig. 5B–C). These results suggested that the administration of CP and K-1 aerial extracts at a dosage at 50 mg/kg did not induce systemic toxicity in mice.

The spleen, being the largest secondary lymphoid organ in the body, serves a critical role in performing a range of immunological functions. It functions as a vital immune effector organ with significant anti-inflammatory activity, regulating both innate and adaptive responses [47]. When antigens or pathogen infect the body, immune-related cells in the spleen are activated and produce various cytokines, including IL-6, IL-1β, and TNF-α to regulate the immune response [48]. Thus, the levels of these cytokines in spleen tissue were explored by elevating ELISA and qPCR method. As shown in Fig. 5D–E, the secretion and gene expression of IL-6, IL-1β, and TNF-α in LPS-injected mice was considerably higher than in the control group. However, the groups administered with CP and K-1 aerial extracts exhibited a potent suppressive effect on these cytokines in LPS-injected mice, surpassing the effect observed in the group administered with DEX.

3.9. Inhibitory effects on MAPKs and NFκB signaling pathways in LPS-injected mice spleen

Subsequently, we examined NFκB and MAPKs signaling pathways to elucidate the underlying mechanism behind the regulation of cytokine secretion and expression by CP and K-1 aerial extracts. Fig. 5F presents that the LPS group exhibited a significant induction of MAPKs and NFκB signaling pathways, as evidenced by increased protein expression levels of *p*-ERK, *p*-JNK, p-p38, *p*-IκBα, and *p*-NFκB compared to the control group. However, the administration of CP and K-1 aerial extracts led to a reduction of protein expressions. Consequently, based on the aforementioned *in vivo* results, K-1 aerial extracts effectively decreased LPS-stimulated inflammatory responses in mice spleen by downregulating the MAPKs and NFκB signaling pathways as well as CP aerial extracts.

4. Conclusion

This study was the first comprehensive attempt to compare the phenotype characteristics and explore the relative content differences of ginsenosides between the stem-and-leaf and root parts of five hydroponically grown ginseng cultivars. Our study highlighted K-1 as a standout cultivar with superior aerial traits and pathogen resistance, making it a highly productive cultivar. After elucidating the chemical composition of both aerial and root extracts, we identified ginsenoside content specifically enriched in the stem-and-leaf, with ginsenoside Rd exhibiting the most abundance. Additionally, K-1 aerial extract exhibited the highest total polyphenol content. Of particular significance, CP and K-1 aerial extracts demonstrated potent anti-inflammatory properties by suppressing the MAPKs and NFκB signaling pathway in LPS-stimulated RAW264.7 macrophages and LPS-induced mice model. Consequently, K-1 aerial extract effectively reduced the secretion and expression of pro-inflammatory mediators and cytokines. In contrast, the aerial extract of the traditional CP cultivar, characterized by poor phenotypic expression and a high percentage of pathogen infection in hydroponic cultivation, showed similar anti-inflammatory efficacy. Taken together, the new K-1 cultivar holds promise for large-scale cultivation for aerial ginsenoside extraction and serves as a potential source and economical alternative for anti-inflammatory agents in dietary interventions. Besides, these results established a chemical foundation for the effective utilization of the aerial parts of hydroponically cultivated ginseng cultivars.

Funding

This work was supported by KDBIO Corp. and the fund of National Research Foundation of Korea (NRF) (2023R1A2C1007606) and -, Rural Development Administration (Project No. PJ01703502), South Korea.

Declarations of competing interests

The authors declare that they have no known competing financial interests or personal relationships that could have appeared to influence the work reported in this paper.

Abbreviations

LPS	lipopolysaccharide
NO	nitric oxide
IL-6	interleukin 6
TNF-α	tumor necrosis factor-alpha
IL-1β	interleukin 1-beta
iNOS	inducible nitric oxide synthase
KP	Kumpoong
CP	Chunpoong
HKJ	Honkaejong
YP	Yunpoong
DEX	Dexamethasone
MitoSOX ROS	Mitochondria Superoxide Reactive Oxygen Species

Appendix A. Supplementary data

Supplementary data to this article can be found online at https://doi.org/10.1016/j.jgr.2024.07.001.

References

[1] Jang HJ, Han IH, Kim YJ, Yamabe N, Lee D, Hwang GS, et al. Anticarcinogenic effects of products of heat-processed ginsenoside Re, a major constituent of ginseng berry, on human gastric cancer cells. J Agric Food Chem 2014;62:2830–6. https://doi.org/10.1021/jf5000776.

[2] Jung S, Lee MS, Shin Y, Kim CT, Kim IH, Kim YS, et al. Anti-obesity and anti-inflammatory effects of high hydrostatic pressure extracts of ginseng in high-fat diet induced obese rats. J Funct Foods 2014;10:169–77. https://doi.org/10.1016/j.jff.2014.06.007.

[3] Hyun SH, Bhilare KD, G, Park CK, Kim JH. Effects of *Panax ginseng* and ginsenosides on oxidative stress and cardiovascular diseases: pharmacological and therapeutic roles. J Ginseng Res 2022;46:33–8. https://doi.org/10.1016/j.jgr.2021.07.007.

[4] Yang L, Zou H, Gao Y, Luo J, Xie X, Meng W, et al. Insights into gastrointestinal microbiota-generated ginsenoside metabolites and their bioactivities. Drug Metab Rev 2020;52:125–38. https://doi.org/10.1080/03602532.2020.1714645.

[5] Hwang JE, Suh DH, Kim KT, Paik HD. Comparative study on anti-oxidative and anti-inflammatory properties of hydroponic ginseng and soil-cultured ginseng. Food Sci Biotechnol 2019;28:215–24. https://doi.org/10.1007/s10068-018-0450-x.

[6] Wang Y, Zhang JJ, Hou JG, Li X, Liu W, Zhang JT, et al. Protective effect of ginsenosides from stems and leaves of *Panax ginseng* against Scopolamine-induced memory damage via multiple molecular mechanisms. Am J Chin Med 2022;50:1113–31. https://doi.org/10.1142/S0192415X22500458.

[7] Choi J, Kim J, Yoon HI, Son JE. Effect of far-red and UV-B light on the growth and ginsenoside content of ginseng (*Panax ginseng* C. A. Meyer) sprouts aeroponically grown in plant factories. Hortic Environ Biotechnol 2022;63:77–87. https://doi.org/10.1007/s13580-021-00380-9.

[8] Kim G, Hyun D, Kim Y, Lee S, Kwon H, Cha S, et al. Investigation of ginsenosides in different parts of *Panax ginseng* cultured by hydroponics. Korean J Hortic Sci Technol 2010;28:216–26.

[9] Chen L, Deng H, Cui H, Fang J, Zuo Z, Deng J, et al. Inflammatory responses and inflammation-associated diseases in organs. Oncotarget 7204 2018;9. www.impactjournals.com/oncotarget.

[10] Furman D, Campisi J, Verdin E, Carrera-Bastos P, Targ S, Franceschi C, et al. Chronic inflammation in the etiology of disease across the life span. Nat Med 2019;25:1822–32. https://doi.org/10.1038/s41591-019-0675-0.

[11] Mohammadi H, Hadi A, Kord-Varkaneh H, Arab A, Afshari M, Ferguson AJR, et al. Effects of ginseng supplementation on selected markers of inflammation: a systematic review and meta-analysis. Phytother Res 2019;33:1991–2001. https://doi.org/10.1002/ptr.6399.
[12] Zhang H, Zhang H, Abid S, Ahn JC, Mathiyalagan R, Kim YJ, et al. Characteristics of *Panax ginseng* cultivars in Korea and China. Molecules 2020;25. https://doi.org/10.3390/molecules25112635.
[13] Kim NH, Choi H Il, Ahn IO, Yang TJ. EST-SSR marker sets for practical authentication of all nine registered ginseng cultivars in Korea. J Ginseng Res 2012;36:298–307. https://doi.org/10.5142/jgr.2012.36.3.298.
[14] Jo IH, Bang KH, Kim YC, Lee JW, Seo AY, Seong BJ, et al. Rapid identification of ginseng cultivars (*Panax ginseng* Meyer) using novel SNP-based probes. J Ginseng Res 2011;35:504–13. https://doi.org/10.5142/jgr.2011.35.4.504.
[15] Lee GO, Jang SN, Kim MJ, Cho DY, Cho KM, Lee JH, et al. Comparison of growth Patterns and Metabolite composition of different ginseng cultivars (Yunpoong and K-1) grown in a Vertical farm. Horticulturae 2023;9. https://doi.org/10.3390/horticulturae9050583.
[16] Wang H, Sun H, Kwon WS, Jin H, Yang DC. A PCR-based SNP marker for specific authentication of Korean ginseng (*Panax ginseng*) cultivar "Chunpoong.". Mol Biol Rep 2010;37:1053–7. https://doi.org/10.1007/s11033-009-9827-5.
[17] Lee JH, Lee JS, Kwon WS, Kang JY, Lee DY, In JG, et al. Characteristics of Korean ginseng varieties of Gumpoong, Sunun, Sunpoong, Sunone, Cheongsun, and Sunhyang. J Ginseng Res 2015;39:94–104. https://doi.org/10.1016/j.jgr.2014.06.007.
[18] Wang H, Xu F, Wang X, Kwon WS, Yang DC. Molecular discrimination of *Panax ginseng* cultivar K-1 using pathogenesis-related protein 5 gene. J Ginseng Res 2019;43:482–7. https://doi.org/10.1016/j.jgr.2018.07.001.
[19] Kwon W-S, Lee M-G, Choi K-T. Breeding process and characteristics of Yunpoong, a new variety of *Panax ginseng* CA Meyer. J Ginseng Res 2000;24:1–7.
[20] Seo J, Lee JS, Shim SL, In JG, Park CS, Lee YJ, et al. Development and authentication of *Panax ginseng* cv. Sunhong with high yield and multiple tolerance to heat damage, rusty roots and lodging. Hortic Environ Biotechnol 2023;64:753–64. https://doi.org/10.1007/s13580-023-00526-x.
[21] Lee S, Lee J. Beneficial bacteria and fungi in hydroponic systems: Types and characteristics of hydroponic food production methods. Sci Hortic 2015;195:206–15. https://doi.org/10.1016/j.scienta.2015.09.011.
[22] Charkowski AO. The changing Face of bacterial soft-rot diseases. Annu Rev Phytopathol 2018;12. https://doi.org/10.1146/annurev-phyto-080417.
[23] Lee GO, Jang SN, Kim MJ, Cho DY, Cho KM, Lee JH, et al. Comparison of growth Patterns and Metabolite composition of different ginseng cultivars (Yunpoong and K-1) grown in a Vertical farm. Horticulturae 2023;9. https://doi.org/10.3390/horticulturae9050583.
[24] Ying Z, Awais M, Akter R, Xu F, Baik S, Jung D, et al. Discrimination of *Panax ginseng* from counterfeits using single nucleotide polymorphism: a focused review. Front Plant Sci 2022;13. https://doi.org/10.3389/fpls.2022.903306.
[25] Kang OJ, Kim JS. Comparison of ginsenoside contents in different parts of Korean ginseng (*Panax ginseng* C.A. Meyer). Prev Nutr Food Sci 2016;21:389–92. https://doi.org/10.3746/pnf.2016.21.4.389.
[26] Lee JY, Yang H, Lee TK, Lee CH, Seo JW, Kim JE, et al. A short-term, hydroponic-culture of ginseng results in a significant increase in the anti-oxidative activity and bioactive components. Food Sci Biotechnol 2020;29:1007–12. https://doi.org/10.1007/s10068-020-00735-5.
[27] Xu XY, Yi ES, Kang CH, Liu Y, Lee YG, Choi HS, et al. Whitening and inhibiting NF-κB-mediated inflammation properties of the biotransformed green ginseng berry of new cultivar K1, ginsenoside Rg2 enriched, on B16 and LPS-stimulated RAW 264.7 cells. J Ginseng Res 2021;45:631–41. https://doi.org/10.1016/j.jgr.2021.02.007.
[28] Yoon D, Choi BR, Kim YC, Oh SM, Kim HG, Kim JU, et al. Comparative analysis of *Panax ginseng* berries from seven cultivars using UPLC-QTOF/MS and NMR-based metabolic profiling. Biomolecules 2019;9. https://doi.org/10.3390/biom9090424.
[29] Li J, Huang Q, Yao Y, Ji P, Mingyao E, Chen J, et al. Biotransformation, Pharmacokinetics, and pharmacological activities of ginsenoside Rd against multiple diseases. Front Pharmacol 2022;13. https://doi.org/10.3389/fphar.2022.909363.
[30] Song X, Wang L, Fan D. Insights into recent studies on Biotransformation and pharmacological activities of ginsenoside Rd. Biomolecules 2022;12. https://doi.org/10.3390/biom12040512.
[31] Kussmann M, Abe Cunha DH, Berciano S. Bioactive compounds for human and planetary health. Front Nutr 2023;10. https://doi.org/10.3389/fnut.2023.1193848.
[32] T S C, J CK, Jku G, M P K, Balachandran I. Phytochemical comparison and evaluation of anti-inflammatory and anti-diabetic activity of three source plants of Jivanti-an important Ayurvedic drug. Futur J Pharm Sci 2021;7. https://doi.org/10.1186/s43094-021-00201-x.
[33] Mæhre HK, Dalheim L, Edvinsen GK, Elvevoll EO, Jensen IJ. Protein determination—method matters. Foods 2018;7. https://doi.org/10.3390/foods7010005.
[34] Aimo J, Promancio E, Damiani PC. Determination of reducing sugars in foodstuff applying multivariate second-order calibration. Anal Methods 2016;8:4617–31. https://doi.org/10.1039/c6ay00964f.
[35] Lam RS, O'Brien-Simpson NM, Holden JA, Lenzo JC, Fong SB, Reynolds EC. Unprimed, M1 and M2 macrophages differentially interact with *Porphyromonas gingivalis*. PLoS One 2016;11. https://doi.org/10.1371/journal.pone.0158629.
[36] Placha D, Jampilek J. Chronic inflammatory diseases, anti-inflammatory agents and their delivery nanosystems. Pharmaceutics 2021;13:1–27. https://doi.org/10.3390/pharmaceutics13010064.
[37] Hussain T, Tan B, Yin Y, Blachier F, Tossou MCB, Rahu N. Oxidative stress and inflammation: what polyphenols can Do for Us? Oxid Med Cell Longev 2016;2016. https://doi.org/10.1155/2016/7432797.
[38] Lee JH, Kim SC, Lee HY, Cho DY, Jung JG, Kang D, et al. Changes in nutritional compositions of processed mountain-cultivated ginseng sprouts (*Panax ginseng*) and screening for their antioxidant and anti-inflammatory properties. J Funct Foods 2021;86. https://doi.org/10.1016/j.jff.2021.104668.
[39] Laavola M, Nieminen R, Leppänen T, Eckerman C, Holmbom B, Moilanen E. Pinosylvin and Monomethylpinosylvin, Constituents of an extract from the Knot of *Pinus sylvestris*, Reduce inflammatory gene expression and inflammatory responses in vivo. J Agric Food Chem 2015;63:3445–53. https://doi.org/10.1021/jf504606m.
[40] Zamora R, Vodovotz Y, Billiar TR. Inducible nitric oxide synthase and inflammatory diseases. 2000.
[41] Tur J, Pereira-Lopes S, Vico T, Marín EA, Muñoz JP, Hernández-Alvarez M, et al. Mitofusin 2 in macrophages Links mitochondrial ROS production, cytokine release, Phagocytosis, Autophagy, and Bactericidal activity. Cell Rep 2020;32. https://doi.org/10.1016/j.celrep.2020.108079.
[42] Rimessi A, Previati M, Nigro F, Wieckowski MR, Pinton P. Mitochondrial reactive oxygen species and inflammation: molecular mechanisms, diseases and promising therapies. Int J Biochem Cell Biol 2016;81:281–93. https://doi.org/10.1016/j.biocel.2016.06.015.
[43] Kraaij MD, van der Kooij SW, Reinders MEJ, Koekkoek K, Rabelink TJ, van Kooten C, et al. Dexamethasone increases ROS production and T cell suppressive capacity by anti-inflammatory macrophages. Mol Immunol 2011;49:549–57. https://doi.org/10.1016/j.molimm.2011.10.002.
[44] Turner MD, Nedjai B, Hurst T, Pennington DJ. Cytokines and chemokines: at the crossroads of cell signalling and inflammatory disease. Biochim Biophys Acta Mol Cell Res 2014;1843:2563–82. https://doi.org/10.1016/j.bbamcr.2014.05.014.
[45] Xiao K, Liu C, Tu Z, Xu Q, Chen S, Zhang Y, et al. Activation of the NF-κ B and MAPK signaling pathways Contributes to the inflammatory responses, but not cell Injury, in IPEC-1 cells Challenged with Hydrogen Peroxide. Oxid Med Cell Longev 2020;2020. https://doi.org/10.1155/2020/5803639.
[46] Tran THM, Puja AM, Kim H, Kim YJ. Nanoemulsions prepared from mountain ginseng-mediated gold nanoparticles and silydianin increase the anti-inflammatory effects by regulating NF-κB and MAPK signaling pathways. Biomater Adv 2022;137. https://doi.org/10.1016/j.bioadv.2022.212814.
[47] Mebius RE, Kraal G. Structure and function of the spleen. Nat Rev Immunol 2005;5:606–16. https://doi.org/10.1038/nri1669.
[48] Lewis SM, Williams A, Eisenbarth SC. Structure and function of the immune system in the spleen. Sci Immunol 2019;4. https://doi.org/10.1126/sciimmunol.aau6085.